Struct Multidisc Optim
DOI 10.1007/s00158-015-1340-y

RESEARCH PAPER

A piezoelectric model based multi-objective optimization of robot gripper design

Rituparna Datta[1] · **Ajinkya Jain**[1] · **Bishakh Bhattacharya**[1]

Received: 30 April 2015 / Revised: 17 August 2015 / Accepted: 11 September 2015

Abstract The field of robotics is evolving at a very high pace and with its increasing applicability in varied fields, the need to incorporate optimization analysis in robot system design is becoming more prominent. The present work deals with the optimization of the design of a 7-link gripper. As actuators play a crucial role in functioning of the gripper, the actuation system (piezoelectric (PZ), in this case) is also taken into consideration while performing the optimization study. A minimalistic model of PZ actuator, consisting different series and parallel assembly arrangements for both mechanical and electrical parts of the PZ actuators, is proposed. To include the effects of connector spring, the relationship of force with actuator displacement is replaced by the relation between force and the displacement of point of actuation at the physical system. The design optimization problem of the gripper is a non-linear, multi modal optimization problem, which was originally formulated by Osyczka (2002). In the original work, however, the actuator was a 'constant output-force actuator model' providing a constant output without describing the internal structure. Thus, the actuator model was not integrated in the optimization study. Four different cases of the PZ modelling have been solved using multi-objective evolutionary algorithm (MOEA). Relationship between force and actuator displacement is obtained using each set of non-dominated solutions. These relationships can provide a better insight to the end user to select the appropriate voltage and gripper design for specific application.

Keywords Robot gripper design · Piezoelectric actuator model · Multi-objective optimization · Mechanism design optimization · Minimalistic model · Series and parallel assembly for mechanical and electrical systems

1 Introduction

Robotic gripper, also known as the end effector, enables a mechanism to interact with the environment mechanically. It is usually attached with the end link of a robotic mechanism and is responsible for converting a mechanism into a manipulator. With the advancement of gripper control technologies, robotic grippers have become a preferential choice in areas requiring high precision and accuracy like automotive industries, aircraft industries, micro and nano fabrication industries. Moreover, as precise control of robotic grippers can be done remotely by using master-slave configurations, they also find use in the areas involving hazardous and high risk operations such as bomb disposal, demining, nuclear fuel handling etc. For more domain specific applications readers are encouraged to read works by Bicchi and Kumar (2000), Reddy and Suresh VS (2013), and Harres (2013).

Actuators are integrated into robot grippers to drive the mechanism and movement control. Different actuators like mechanical, electrico-hydraulic, pneumatic and hybrid actuators are generally used in robotic grippers. However, since

✉ Bishakh Bhattacharya
bishakh@iitk.ac.in

Rituparna Datta
rdatta@iitk.ac.in

Ajinkya Jain
ajinkya@iitk.ac.in

[1] Smart Materials Structure and Systems Lab, Department of Mechanical Engineering, Indian Institute of Technology Kanpur, Kanpur, PIN 208016, India

Published online: 15 October 2015

last few years the usage of smart actuators has attracted the attention of both industries and research community as a promising alternative solution. Smart actuators have found extensive use in high precision and light weight applications. These actuators are generally based on PZ materials, shape memory alloy, magneto-strictive materials, electroactive polymers and magneto rheological fluid.

In the present work, an optimization study has been carried out to optimize the performance of PZ actuator based gripper systems. The gripper for the present work is an extended version of the work originally formulated by Osyczka (2002). In the original formulation (Osyczka (2002)), actuator was considered as a 'constant output-force actuator model', providing a constant output and the actuator internal structure/ transfer function was ignored. However, as actuator plays the most critical role, by supplying actively controlled force and displacement to the gripper, it must be also taken into account while performing an optimization study for the gripper mechanism. To alleviate the aforementioned limitation in Osyczka (2002), a voice-coil type actuation system is introduced in Shikhar (2014).

PZ actuators consume low power and have shorter response time, higher size to output force ratio, and better controllability in comparison to conventional actuators. Because of such properties, PZ actuators are gaining significant attention from both academia and industries, specifically for micro and nano-scale operations. In works by Goldfarb and Celanovic (1999), Pérez et al. (2005), and Zubir et al. (2009), various usage of PZ actuators for micro-scale applications have been discussed. However, by nature, (PZ) materials show a coupling of electrical and mechanical properties of materials. In the present work, a PZ actuation system is considered due to its superior performance in comparison to the traditional actuators.

With increasing interest in PZ actuators, numerous models of the voltage responses of PZ actuators have been developed in past few decades ((Low and Guo 1995; Adriaens et al. 2000; Gu et al. 2013)). A review on various models developed in relation with PZ actuators for intelligent structures was done by Chee et al. (1998). Some further reviews on PZ actuator usage and modeling can be found in Benjeddou (2000), Irschik (2002), and Anton and Sodano (2007). Adriaens et al. (2000) considered first order differential equation to describe the hysteresis effect and used a partial differential equation to describe the mechanical behavior of the PZ actuator. Similar models and their usage in various applications also have been discussed in Croft and Devasia (1998) and Tzen et al. (2003). In Croft and Devasia (1998) and Tzen et al. (2003), cascaded models have been used to model the hysteresis non-linearity; while the former work decoupled hysteresis and structural dynamics, the latter separated linear and non-linear parts of the actuator dynamics. Using a complex model of actuator (PZ, in this case) in the optimization study, may significantly increase the already high computational cost, which is undesirable. On the other hand, treating actuator as a simple 'constant output-force actuator model' in the study, will make the study less accurate and hence less effective. To tackle the problem of actuator modeling, a minimalistic model of PZ actuator have been developed by the authors. In this minimalistic mode, various series and parallel combinations of springs and capacitors, representing mechanical and electrical domains respectively, have been proposed. Based on the specific engineering application requirement, a particular spring-capacitor assembly can be used. Usage of linearized constitutive equations in the model, makes it computationally cheaper while maintaining its effectiveness. Hence, the proposed minimalistic model becomes an ideal choice for this optimization study.

Some detailed studies addressing the design optimization of robot gripper mechanisms using various optimization techniques, can be found in Krenich (2004). In Ciocarlie and Allen (2010), gripper design optimization for an underactuated gripper, has been explored. While in another recent work (Ciocarlie et al. 2014), two strategies of optimization for a two-finger, single-actuator gripper has been developed. Aim of the study was to ensure stability and extend the range of objects to be gripped. In the present work, actuator modelling is integrated into a multi-objective optimization problem initially formulated by Osyczka (2002). Multi-objective Genetic Algorithm (GA) is used to solve the optimization problem. The original optimization problem, without taking into account actuator analysis, have also been solved by many researchers (Osyczka et al. (1999), Saravanan et al. (2009), and Datta and Deb (2011)).

This paper is divided into five further sections. In Section 2, mechanical design of the gripper is discussed. The optimization problem formulation and constraints are discussed in Appendix A and the results of innovization[1] study from previous work done by Datta and Deb (2011) in are shown in Appendix B. Section 3 discusses the minimalistic PZ actuator modelling proposed, while results of the optimization study are presented in Section 4. Piezoelectric modelling and results are discussed in Section 5, and Section 6 concludes the present work.

2 Mechanical design of gripper

The gripper design problem is solved using evolutionary algorithm in the present work. The original multi-objective optimization problem (Osyczka 2002) considered two conflicting objectives: the minimization of range of gripping

[1]The term Innovization refers to the process of innovation as a result of optimization study.

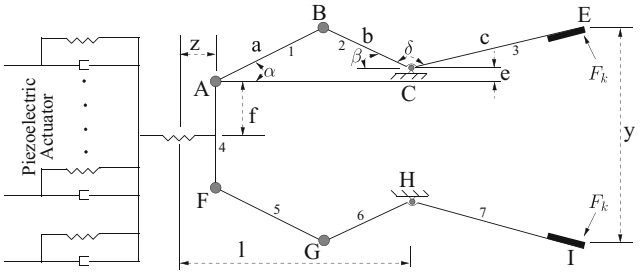

Fig. 1 Figure depicting the mechanical design of the robotic gripper used in current study (taken from Osyczka (2002) and integrated with PZ actuator)

force and maximization of output-input force ratio. The variables in the optimization process are link lengths and joint angles. Constraints are imposed on the force delivered by the gripper along with the variables. The gripper in study is a seven-link mechanism, shown in Fig. 1. In the gripper assembly, link 2 and link 3 are rigidly joined at a fixed angle δ and combined link is pivoted to the ground. Similarly, link 6 and 7 are joined and are pivoted. The gripping action is provided by the relative motion between link 3 and link 7.

The problem formulation of the robot gripper design is as follows:

$$
\begin{aligned}
&\text{Minimize} \quad F_1(\mathbf{x}) = \max_z F_k(\mathbf{x}, z) - \min_z F_k(\mathbf{x}, z),\\
&\text{Minimize} \quad F_2(\mathbf{x}) = \frac{P}{\min_z F_k(\mathbf{x}, z)},\\
&\text{Subject to} \quad g_1(\mathbf{x}) = Y_{\min} - y(\mathbf{x}, Z_{\max}) \geq 0,\\
&\qquad g_2(\mathbf{x}) = y(\mathbf{x}, Z_{\max}) \geq 0,\\
&\qquad g_3(\mathbf{x}) = y(\mathbf{x}, 0) - Y_{\max} \geq 0,\\
&\qquad g_4(\mathbf{x}) = Y_G - y(\mathbf{x}, 0) \geq 0,\\
&\qquad g_5(\mathbf{x}) = (a+b)^2 - l^2 - e^2 \geq 0,\\
&\qquad g_6(\mathbf{x}) = (l - Z_{\max})^2 + (a-e)^2 - b^2 \geq 0,\\
&\qquad g_7(\mathbf{x}) = l - Z_{\max} \geq 0,\\
&\qquad g_8(\mathbf{x}) = \min_z F_k(\mathbf{x}, z) - FG \geq 0,\\
&\qquad 10 \leq a,\ b,\ f \leq 250,\\
&\qquad 10 \leq a,\ b,\ f \leq 250,\\
&\qquad 100 \leq c \leq 300,\\
&\qquad 0 \leq e \leq 50,\\
&\qquad 10 \leq f \leq 250,\\
&\qquad 100 \leq l \leq 300,\\
&\qquad 1.0 \leq \delta \leq 3.14.
\end{aligned}
\tag{1}
$$

The details of the robot gripper design formulation is shown in Appendix A. In our problem formulation, it is evident that the two formulated objective problems are mutually conflicting. The first objective function minimizes the difference between the maximum and minimum values of gripping force. As the value of maximum gripping force will be quite high in general, the first objective function tends to maximize the minimum gripping force. As the value of minimum gripping force maximizes, the whole set of gripping force values maximizes, i.e. the gripping force maximizes. However, it is evident from the second objective function that in order to maximize the force transformation ratio, a lower value of gripping force is suitable. Therefore,

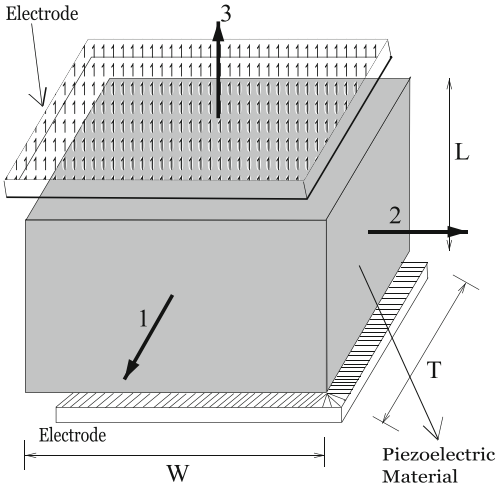

Fig. 2 Illustration of PZ stack in three dimensional space. Voltage is applied along direction 3 and in the stack configuration displacement is also obtained along direction 3

the two objective functions are conflicting with each other and the use of multi-objective optimization is required in our analysis.

3 Actuator modeling: piezoelectric actuator

The constitutive relationships published in IEEE standard (1987), constitutes linear equations explaining the electromechanical coupling of PZ materials. These equations are the governing equations of the proposed minimalistic model of PZ actuator (Jain et al. 2015). The relationships in matrix form are as following:

$$
\begin{bmatrix} \mathbf{D}_{3\times1} \\ \mathbf{S}_{6\times1} \end{bmatrix} = \begin{bmatrix} \mathbf{d}_{3\times6} & \boldsymbol{\epsilon}^{\sigma}_{3\times3} \\ \mathbf{s}^{E}_{6\times6} & \mathbf{d}^{t}_{6\times3} \end{bmatrix} \times \begin{bmatrix} \boldsymbol{\sigma}_{6\times1} \\ \mathbf{E}_{3\times1} \end{bmatrix} \tag{2}
$$

where,

D : electric displacement field vector
S : mechanical strain vector
$\boldsymbol{\sigma}$: mechanical stress vector
E : applied electric field intensity

Table 1 Examples of commercially available PZ actuators with characteristic properties

Characteristic property	Commercial PZ actuator examples
High mechanical compliance	P-601, P-602, P-603, P-604 PiezoMove series
High mechanical stiffness	P-882 P-888 PICMA
Low response time	P-885.55, P-885.95, P-888.55 encapsulated PICMA
High robustness to electrical disturbances	N-470, N-470.V, E-870 PiezoMike

Table 2 Numerical force - actuator displacement relationships for the four cases

		Electrical system	
		Series	Parallel
Mechanical system	Series	$F_{st} = \frac{z + d_{33} V_{st}}{\left(\frac{1}{k_{con}} + \frac{nL}{E_p A}\right)}$	$F_{st} = \frac{z + d_{33} n V_{st}}{\left(\frac{1}{k_{con}} + \frac{nL}{E_p A}\right)}$
	Parallel	$F_{st} = \frac{z + \frac{d_{33} V_{st}}{n}}{\left(\frac{1}{k_{con}} + \frac{L}{E_p n A}\right)}$	$F_{st} = \frac{z + d_{33} V_{st}}{\left(\frac{1}{k_{con}} + \frac{L}{E_p n A}\right)}$

$\mathbf{d}$: PZ charge constant (shows intensity of PZ effect)
$\boldsymbol{\epsilon}^{\sigma}$: dielectric constant of PZ material at const. σ
$\mathbf{s}^{E}$: electric compliance for a constant E
$\mathbf{d}^{t}$: transpose of the PZ charge constant matrix

As the main direction of actuation will be along the longitudinal direction (direction 3 in Fig. 2), the variations along other directions can be neglected. Hence, the matrix (2) reduces to simplified algebraic equations as follows:

$$D_3 = d_{33}\sigma_3 + \epsilon_{33} E_3. \tag{3}$$

$$S_3 = \frac{1}{E_p}\sigma_3 - d_{33} E_3. \tag{4}$$

where considering plane stress assumption, $\mathbf{s}_{33}^{E} = \frac{1}{E_p}$, E_p being the modulus of elasticity of PZ material.

Again, as the unidirectional displacements will be small, the mechanical stress, strain and electric field strength can be approximated as:

$$\epsilon = \frac{\Delta L}{L}. \tag{5}$$

$$\sigma = \frac{F}{A}. \tag{6}$$

$$E = \frac{V}{L}. \tag{7}$$

where,

L : length along actuation direction (direction 3)

Table 3 Properties and dimensions of the PZ stack actuator used in simulations

d_{33}	=	3.74×10^{-10}	C/N
ϵ_{33}	=	1.505×10^{-8}	C/m^2
E_p	=	$1/1.64 \times 10^{-11}$	Pa
L	=	10	μm
A	=	4	μm^2
k_{con}	=	4×10^5	N/m

A : normal cross-sectional area
F : Force of actuation
V : applied voltage

By substituting the values from (5), (6), (7) into (3) can be reduced to:

$$D_3 = d_{33}\left(\frac{F}{A}\right) + \epsilon_{33}\left(\frac{V}{L}\right). \tag{8}$$

$$\Delta L = \left(\frac{1}{E_p}\right)\left(\frac{F}{A}\right) L - d_{33} V. \tag{9}$$

The proposed PZ actuator model decouples the electrical and mechanical domains of PZ material, by modeling electrical domain of material as a combination of capacitors and mechanical domain as a combination of springs. In the model, four different assemblies (*series and parallel*) of capacitors and springs have been proposed. The PZ actuators showing higher mechanical compliance should be modelled as a series assembly of springs; whereas, those with higher stiffness can be modelled with a parallel assembly of springs. In the electrical domain, PZ actuators having faster response time should be modelled with a series assembly of the capacitors; while those showing higher robustness to electrical disturbances can be modelled

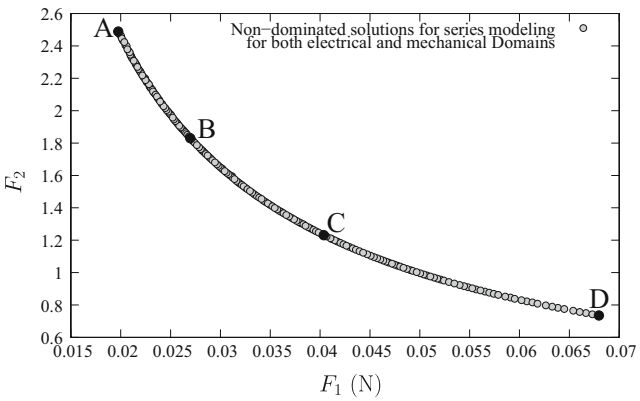

Fig. 3 Non-dominated solutions obtained using NSGA-II for series modeling for both electrical and mechanical domains

Table 4 Extreme and intermediate non-dominated solutions with corresponding design variable values

Points in	Objective functions		Design variables						
Fig. 3	F_1	F_1	a	b	c	e	f	l	δ
A	0.02	2.50	241.35	152.71	109.52	46.65	57.66	101.20	1.71
B	0.03	1.83	244.97	160.76	100.65	49.69	50.59	100.01	1.86
C	0.04	1.23	249.32	177.80	100.38	47.57	60.62	100.00	1.99
D	0.07	0.73	248.04	219.41	100.32	15.77	37.10	100.00	1.68

as a parallel assembly of capacitors. Some of the examples of commercially available PZ actuators with characteristic properties resembling the series and parallel assemblies are given in Table 3. Through the combinations of different assemblies in the two domains, four separate cases for PZ actuator modelling have been proposed. For each assembly, force and voltage relationships have been derived based on the constitutive governing equations.

A salient feature of the proposed PZ actuator model (Jain et al. 2015) is that, it also takes in consideration the connection between the stack assembly and mechanism, in the model itself. The connection has been modeled as a connector spring. Taking L_{st} as the length of the PZ stack, ΔL_{st} as the change in length of the PZ stack, k_{con} as the stiffness of the connection between PZ stack and physical system and z as the displacement at the point of actuation of physical system, the force delivered by the PZ stack F_{st} to the physical system can be given as :

$$F_{st} = k_{con}(z - \Delta L_{st}), \tag{10}$$

$$\Delta L_{st} = z - \frac{F_{st}}{k_{con}}. \tag{11}$$

The effective axial stiffness of the connector spring k_{con} can be calculated as

$$k_{con} = \frac{AE}{L_o} \tag{12}$$

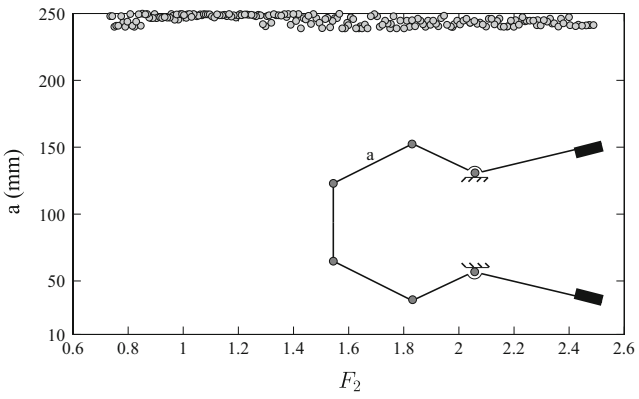

Fig. 4 Variation of link length a with the second objective function (force transformation ratio)

where,

A : cross-sectional area of the actuator assembly
E : Young's Modulus of connector material
L_o : initial length of the connector

The proposed model provide relationships of the force delivered by the stack, with the displacements observed at the actuation point on mechanism and the input voltage required. For each of the four assemblies, Force relationships with the displacement at the actuation point and Voltage are described below (Table 1)[2].

Case A: series modeling for both electrical and mechanical domains When both the electrical and mechanical parts of PZ actuator have been modeled as series assemblies of capacitors and springs respectively, then the total applied external voltage across actuator stack composed of 'n' PZ elements, V_{st} can be given as:

$$V_{st} = nV, \tag{13}$$

The force delivered by PZ stack actuator, F_{st} and the net displacement of the stack, ΔL_{st} is given by:

$$F_{st} = F, \tag{14}$$

$$\Delta L_{st} = n\Delta L, \tag{15}$$

where,

V : voltage across each element,
F : force delivered by each element
ΔL : displacement of each element

Upon substituting the values from (13) and (15) in (9), one may express the net stack displacement as:

$$\Delta L_{st} = \left(\frac{1}{E_p}\right)\left(\frac{F_{st}}{A}\right)nL - d_{33}V_{st}. \tag{16}$$

Further, using (11) and (16), one may obtain F_{st} as:

$$F_{st} = \frac{z + d_{33}V_{st}}{\left(\frac{1}{k_{con}} + \frac{nL}{E_pA}\right)} \tag{17}$$

[2]All serial numbers refer to the respective product numbers of the company Physik Instrumente (PI) GmbH & Co. KG, Germany

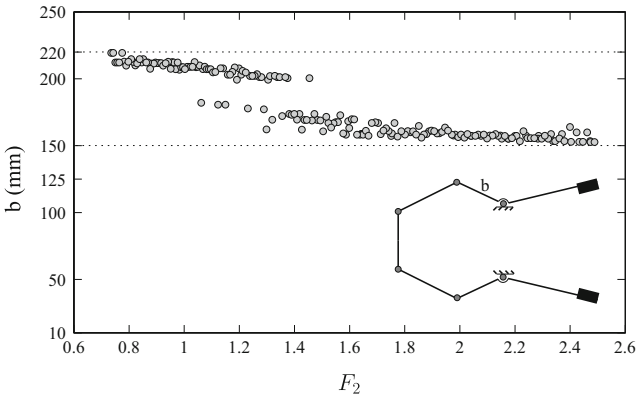

Fig. 5 Variation of link length b with the second objective function (force transformation ratio)

The relationship between F_{st} and z can also be expressed as

$$F_{st} = \alpha_1 z + \beta_1 V_{st}$$
$$where \quad \alpha_1 = \frac{1}{\left(\frac{1}{k_{con}} + \frac{nL}{E_p A}\right)}, \quad \beta_1 = d_{33}\alpha_1 \tag{18}$$

Case B: series modeling for electrical and parallel modeling for mechanical domains For the case of series modelling for electrical part and parallel modelling for mechanical part, the total applied external voltage across actuator stack V_{st}, the force delivered by it F_{st} composed of 'n' PZ elements and the net displacement of actuator ΔL_{st} can be given as:

$$V_{st} = nV. \tag{19}$$

$$F_{st} = nF. \tag{20}$$

$$\Delta L_{st} = \Delta L. \tag{21}$$

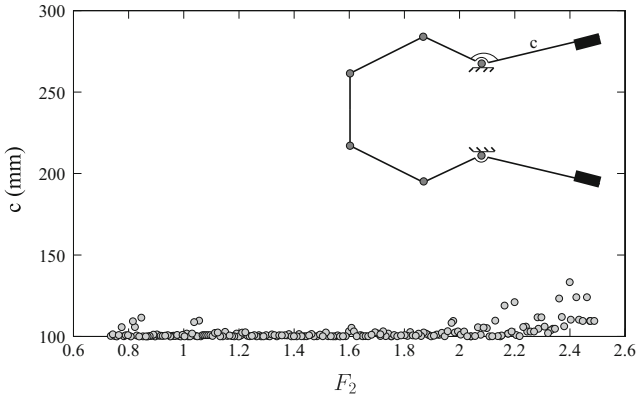

Fig. 6 Variation of link length c with the second objective function (force transformation ratio)

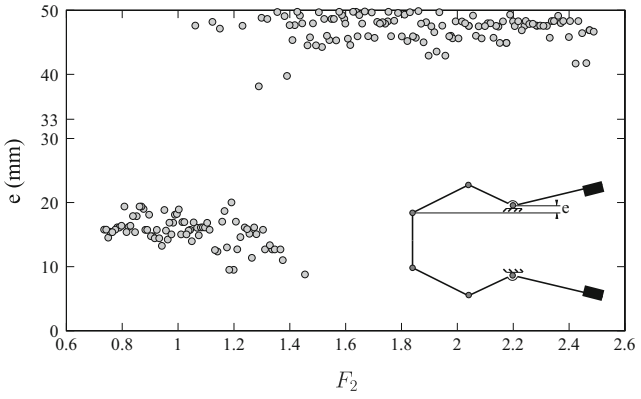

Fig. 7 Variation of offset e with the second objective function (force transformation ratio)

Substituting values from (19), (20), (21) in (9) to obtain:

$$\Delta L_{st} = \left(\frac{1}{E_p}\right)\left(\frac{F_{st}}{nA}\right) L - d_{33}\frac{V_{st}}{n} \tag{22}$$

Further, equating (22) with (11), one may obtain the relation between F_{st} and z as

$$F_{st} = \alpha_2 z + \beta_2 V_{st}$$
$$where \quad \alpha_2 = \frac{1}{\left(\frac{1}{k_{con}} + \frac{L}{E_p nA}\right)}, \quad \beta_2 = \frac{d_{33}}{n}\alpha_2 \tag{23}$$

Case C: parallel modeling for electrical and series modeling for mechanical domains In case of parallel modeling for electrical part and series modeling for mechanical part of the PZ actuator, the applied voltage across actuator V_{st}, the force delivered F_{st} and the stack actuator displacement L_{st} composed of 'n' PZ elements, can be written as:

$$V_{st} = V. \tag{24}$$

$$F_{st} = F. \tag{25}$$

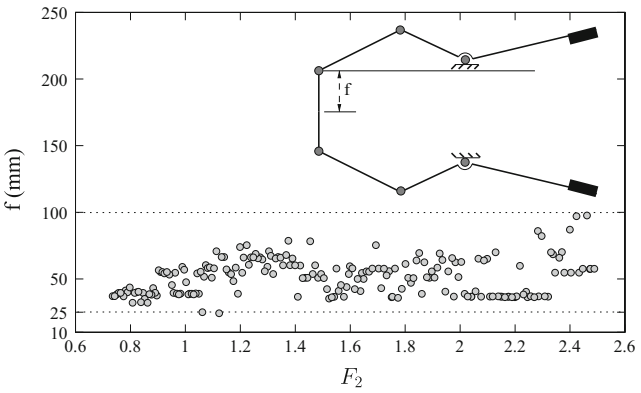

Fig. 8 Variation of offset f with the second objective function (force transformation ratio)

$$\Delta L_{st} = n\Delta L, \tag{26}$$

Substituting (24), (25), (26) in (9), we get

$$\Delta L_{st} = \left(\frac{1}{E_p}\right)\left(\frac{F_{st}}{A}\right) nL - nd_{33}V_{st}. \tag{27}$$

Following a similar procedure, the relation between F_{st} and z can be written as

$$F_{st} = \alpha_3 z + \beta_3 V_{st}$$
$$where \quad \alpha_3 = \frac{1}{\left(\frac{1}{k_{con}} + \frac{nL}{E_p A}\right)}, \quad \beta_3 = nd_{33}\alpha_3 \tag{28}$$

Case D: parallel modeling for both electrical and mechanical domains Considering parallel assemblies of capacitors and springs to represent electrical and mechanical domains of PZ actuator respectively, the applied voltage across actuator V_{st}, the force delivered by it F_{st} composed of 'n' PZ elements, and the stack actuator displacement L_{st}, can be given as:

$$V_{st} = V. \tag{29}$$

$$F_{st} = nF. \tag{30}$$

$$\Delta L_{st} = \Delta L. \tag{31}$$

Equations (29), (30), (31) can be substituted in (9) to obtain

$$\Delta L_{st} = \left(\frac{1}{E_p}\right)\left(\frac{F_{st}}{nA}\right) L - d_{33}V_{st}. \tag{32}$$

Again, the relation between F_{st} and z can be written as

$$F_{st} = \alpha_4 z + \beta_4 V_{st}$$
$$where \quad \alpha_4 = \frac{1}{\left(\frac{1}{k_{con}} + \frac{L}{E_p nA}\right)}, \quad \beta_4 = d_{33}\alpha_4 \tag{33}$$

The proposed mathematical formulations described in this section are summarized in Table 2.

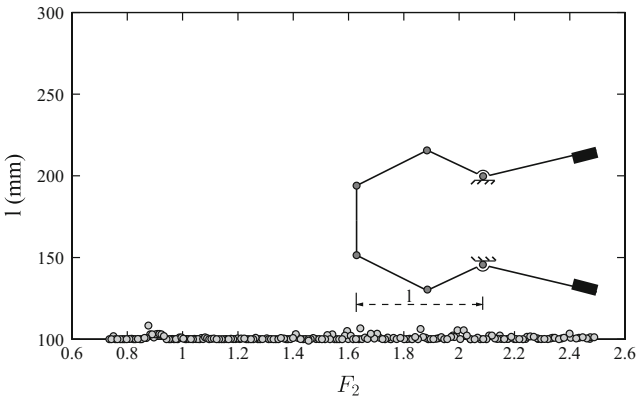

Fig. 9 Variation of offset l with the second objective function (force transformation ratio)

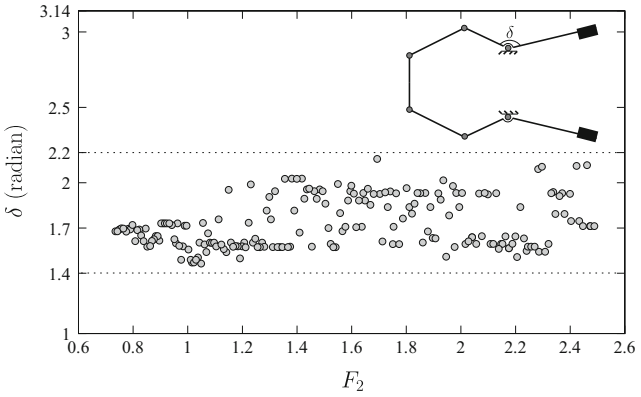

Fig. 10 Variation of joint angle δ with the second objective function (force transformation ratio)

4 Gripper design optimization and results

In the last two sections, we have discussed the proposed PZ model for four different cases and the integration of PZ modelling with the robot gripper design to form four different multi-objective optimization problems. Thence formed multi-objective gripper design problem can be solved using any multi-objective optimization approach. It may be noted that, all objectives must be conflicting in case of a multi-objective optimization problem. As the objectives are more than one and conflicting, the set of feasible solutions will be more than one. Among these feasible solutions, if the designer wants an improvement in one objective, he has to sacrifice another and vice versa. All these solutions are of equal importance and no one dominates the other. The set of all these feasible solutions are called non-dominated solutions.

Due to the nature of multi-modal, non-linear and non-convex objectives and constraints in the gripper design optimization problem, classical multi-objective optimization is not suitable for the four formulated cases. Non-dominated Sorting Genetic Algorithm-II (NSGA-II) (Deb

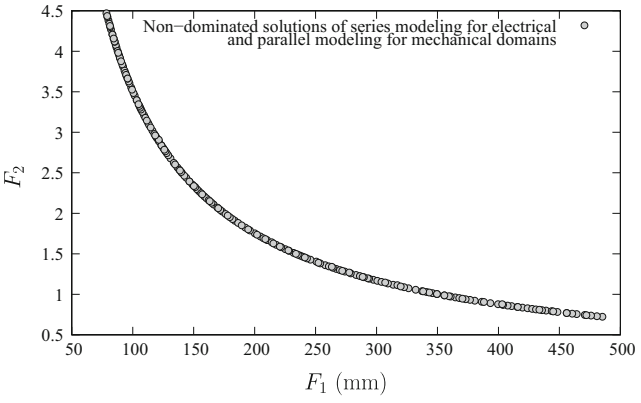

Fig. 11 Non-dominated solutions obtained using NSGA-II for both series modeling for both electrical and mechanical domains

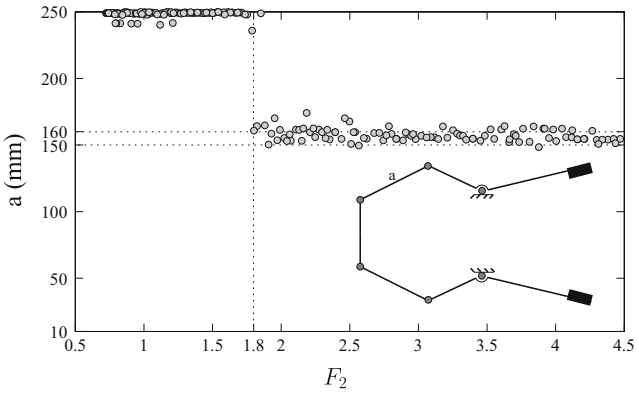

Fig. 12 Variation of link length a with force transformation ratio (second objective function)

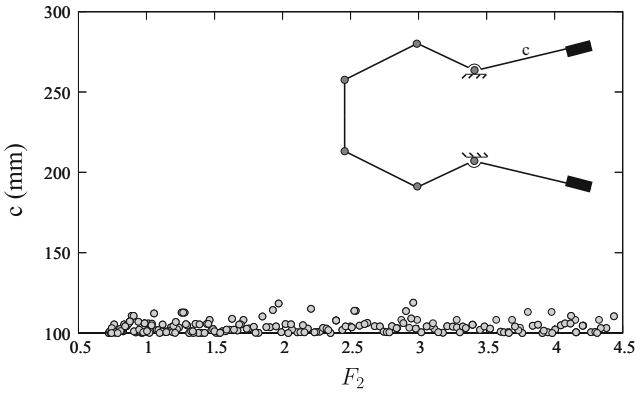

Fig. 14 Variation of link length c with force transformation ratio (second objective function)

et al. (2002)) is used due to its suitability in solving complex multi-objective problems.

The parameters for NSGA-II are as follows:

Population size = 200,
Number of Generations = 10 million,
SBX probability= 0.9,
Polynomial mutation probability = $1/N$,
(N = number of variables),
SBX index = 10, and
Mutation index = 100.

In the proposed actuator modelling (Jain et al. (2015)), F_{st} is given as a function of two independent variables V_{st} and z. However for practical purposes, a relation between V_{st} and z can be derived from experimental data. From the simulation results for a PZ stack actuator with properties and dimensions provided in Table 3. A relationship between V_{st} and z can be formulated as follows:

$$\begin{aligned} V_{st} &= Az + B, \\ where, \quad A &= 3.5245 \times 10^9, \quad B = -366.34, \end{aligned} \tag{34}$$

The problem is solved for four cases of PZ actuators. A relationship between force and voltage can be obtained using each set of non-dominated solutions. The user can choose the voltage based on requirement.

Case A: series modeling for both electrical and mechanical domains The non-dominated solutions between both objective functions are shown in Fig. 3.

The point in the extreme left side of Fig. 3 represents lowest value of first objective function (range of gripping force) and similarly the extreme point on the right side has the lowest second objective function value (force transformation ratio). Based on criteria, an user can choose a point on the non-dominated solutions. Table 4 shows extremes and two intermediate objective functions with corresponding variable values. For example, if a designer chooses the first set of objective values in Table 4, the gripper can be made with corresponding variable values. The same can be repeated for the whole set of non-dominated solutions shown in Fig. 3. These points are also shown in Fig. 3.

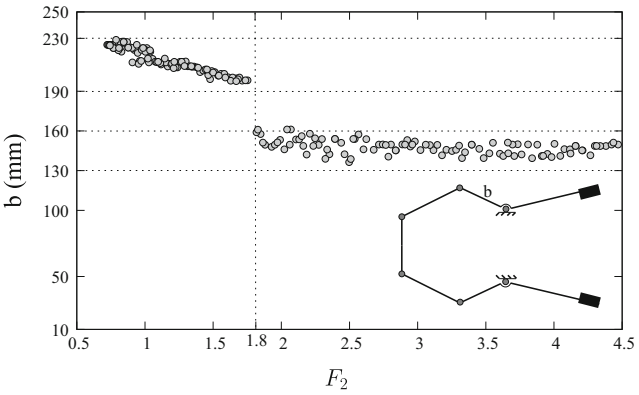

Fig. 13 Variation of link length b with force transformation ratio (second objective function)

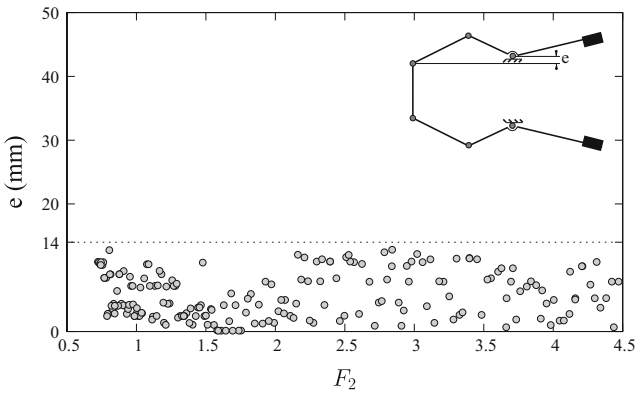

Fig. 15 Variation of offset e with force transformation ratio (second objective function)

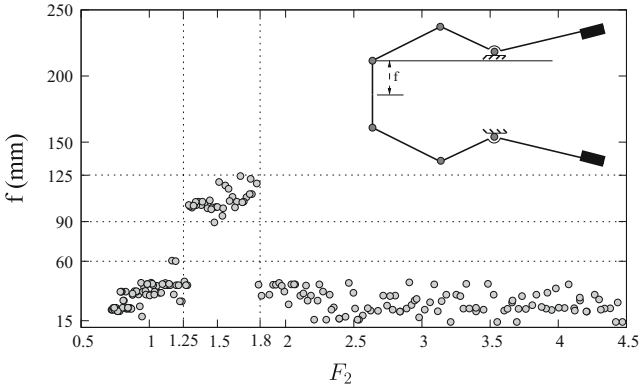

Fig. 16 Variation of offset f with force transformation ratio (second objective function)

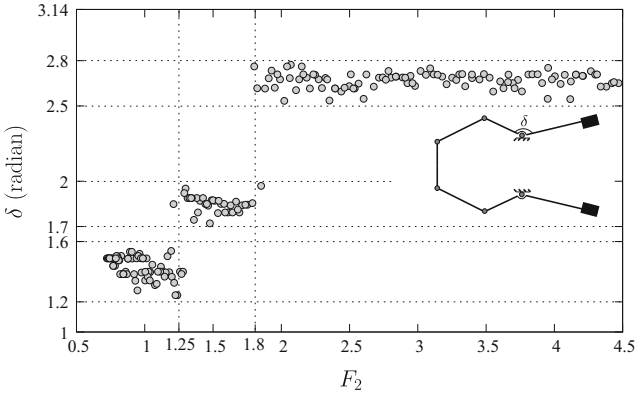

Fig. 18 Variation of joint angle δ with force transformation ratio (second objective function)

4.0.1 Innovization study

In this section the non-dominated solutions are analysed to establish some meaningful relationships between objective functions and design variables. This is known as *innovization* study (Deb and Srinivasan (2006)). To perform *innovization* task, the second objective function is selected and it is plotted against each variables. Figures 4, 5, 6, 7 to 10 show the results of *innovization*.

Figure 4 clearly shows that a (link length) must be fixed to its upper bound. For clear visibility, the link length a is also added in the figure with the gripper. Based on the problem formulation, the upper bound of a is 250 mm. For the present configuration, value of a should be 250 mm.

The relationship between link length b and force transformation ratio is shown in Fig. 5. Figure 5 clearly shows that the variation of link length b is between $150 - 220$ mm. A clear relation between b and force transmission ratio cannot be obtained.

Figure 6 contains the gripper (emphasized link c) and the relationship between second objective function and link length c. The link length c takes the lower bound for most non-dominated solutions. The link c should be fixed at its lower bound.

The offset e shows two regions of concentration, one in between $10 - 20$ mm and another near the upper bound. For better understanding the gripper schematic diagram is also merged with the relationship between offset e and force transformation ratio.

The relationship between offset f and second objective function is shown in Fig. 8. The variation of offset f is restricted to a region between $25 - 100$ mm with a higher concentration near 50 mm. The designer may choose to keep the value of f at 50 mm.

Figure 9 depicts that in most non-dominated solutions the value of offset l occurs to its lower bound. As the variation is negligible, the offset l must be fixed to its lower bound. The joint angle delta can be varied between $1.4 - 2.2$ radians as shown in Fig. 10.

Case B: series modeling for electrical and parallel modeling for mechanical domains Figure 11 shows the Pareto-optimal solutions between the range of gripping force and force transformation ration.

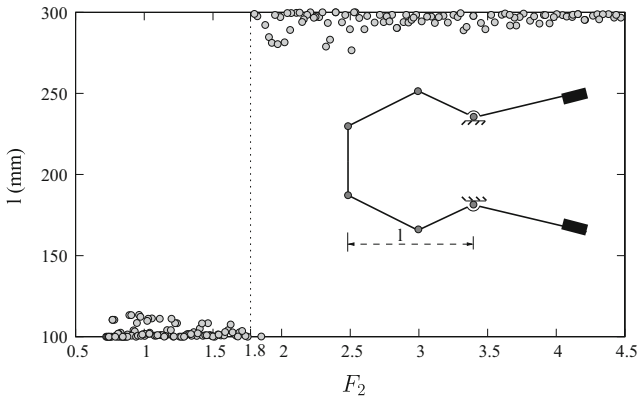

Fig. 17 Variation of offset l with force transformation ratio (second objective function)

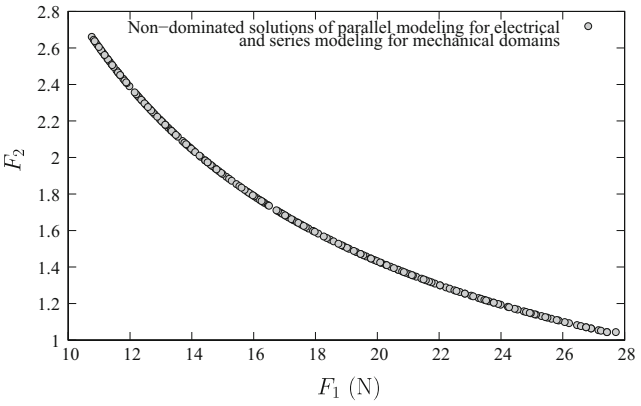

Fig. 19 Non-dominated solutions obtained using NSGA-II for both series modeling for both electrical and mechanical domains

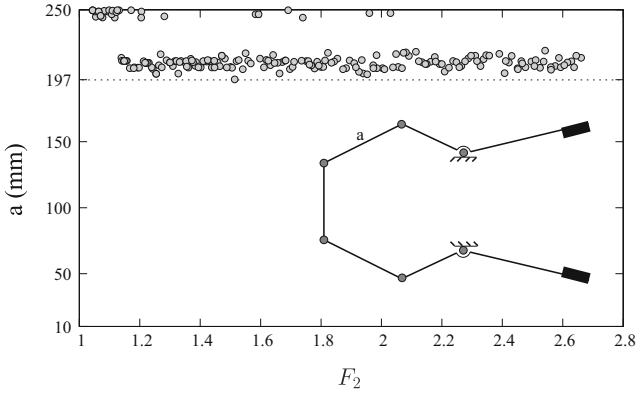

Fig. 20 Variation of link length a with the second objective function (force transformation ratio)

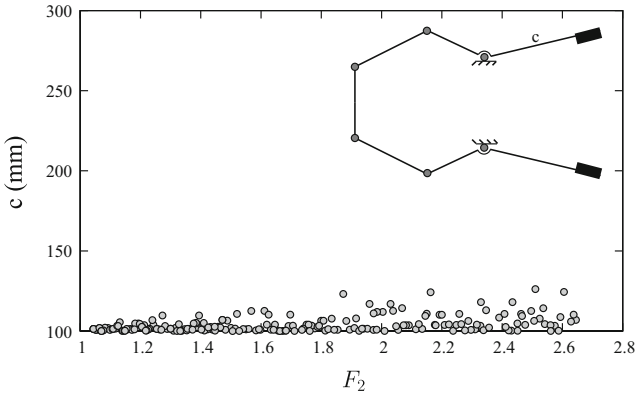

Fig. 22 Variation of link length c with the second objective function (force transformation ratio)

4.0.2 Innovization study

The results of *innovization* study is presented from Figs. 12 to 18.

From Fig. 12, it can be inferred that the optimal value of a (link length) varies between $150 - 250$ mm with two regions of concentration. For values of force transmission ratio less then 1.8, the value of a lies near the upper bound and hence should be chosen as the upper bound value i.e. 250 mm. While for transmission ratio values higher than 1.8, the optimal value should be taken as 160 mm.

The variation of second link length of the mechanism i.e. link length b with the force transformation ratio is shown in Fig. 13. The plot shows banded variation with first band of values varying between $130 - 160$ mm, while second band between $190 - 230$ mm. A fixed value of b throughout the changes in force transformation ratio cannot be obtained.

In Fig. 14, the relationship between the link length c and second objective function is plotted. It can be inferred from the plot that if we neglect some minor variations, the optimal value for the link length c can be taken as the value of lower bound i.e. 100 mm.

The value of offset e varies between $0 - 14$ mm with the second objective function i.e. the transmission ratio, as can be seen in Fig. 15. Hence, no definite relationship can be ascertained between e and the second objective function. Based on the plot shown in Fig. 16, no definite relationship can be obtained between the offset f and the transmission ratio. However, it can be deduced from the plot that for the values of force transmission ratio (F_2) between $1.25 - 1.8$, it would be better to choose a value of f in the range $90 - 125$ mm. For other values of F_2, the range for variation of f is between $15 - 60$ mm.

Figure 17 shows the variation of offset l with force transmission ratio. The trend is similar to that of link length a. For the values of transmission ratio greater than 1.8, value of l is concentrated near the upper bound (300 mm). For lower values, value of l can be fixed at 100 mm (the lower bound).

Since there are large variations in the value of joint angle δ, as evident from Fig. 18, a definite value of the joint angle δ cannot be determined. Three main regions of concentrations i.e. between $1.2 - 1.6$ radians, $1.7 - 2$ radians and $2.5 - 2.8$ radians, are evident from the plot for the values of $F_2 < 1.25$, between $1.25 - 1.8$ and > 1.8 respectively.

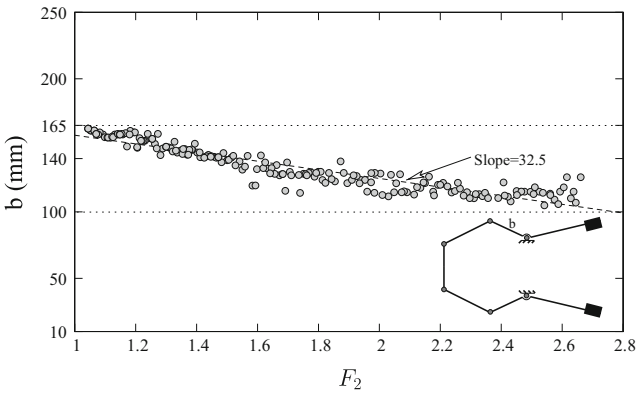

Fig. 21 Variation of link length b with the second objective function (force transformation ratio)

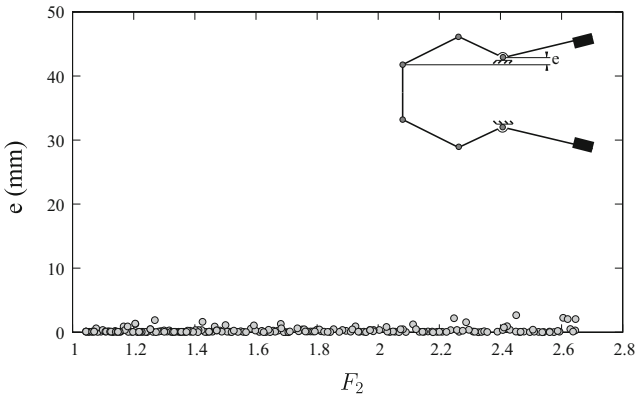

Fig. 23 Variation of offset e with the second objective function (force transformation ratio)

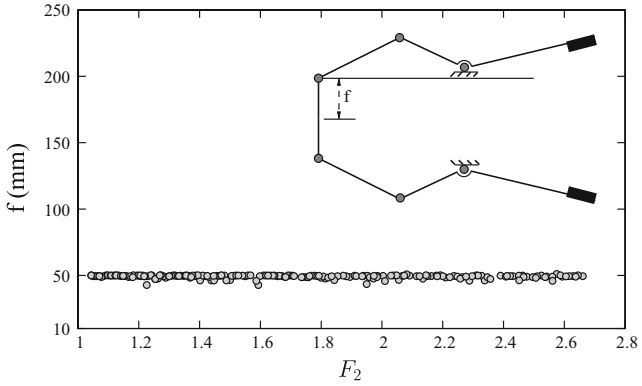

Fig. 24 Variation of offset f with the second objective function (force transformation ratio)

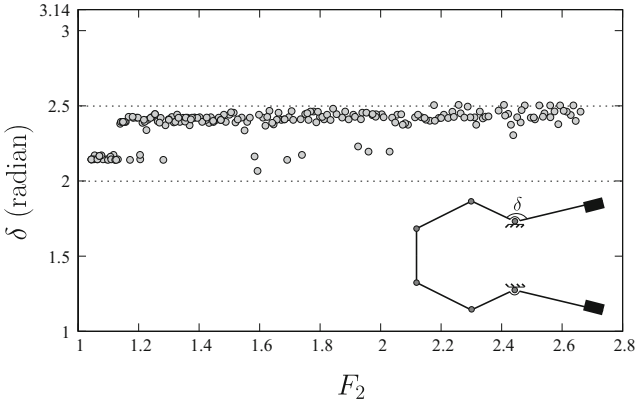

Fig. 26 Variation of joint angle δ with the second objective function (force transformation ratio)

Case C: parallel modeling for electrical and series modeling for mechanical domains The results of the optimization study considering the modelling of case C, are shown in Fig. 19.

4.0.3 Innovization study

The results of *innovization study* are shown in Figs. 20, 21, 22, 23, 24, 25 and 26. In Fig. 20, link length a shows variations in the range $197 - 250$ mm. No definite relationship holding for the entire range of F_2 can be obtained.

Figure 21 depicts the variations in link length b with the force transformation ratio. Link length b varies within a range of $100 - 165$ mm approximately with an average slope of -32.5 and an intercept of 165 mm. Hence, appropriate value of b can be chosen based of the required force transmission ratio.

The plot in Fig. 22 captures the behaviour of link length c with the changes in second objective function of the problem. Apart for a few variations, the value of c is fairly concentrated at the lower bound. Hence, c can be taken as the lower bound value i.e. 100 mm.

Figures 23 and 24 show the plots of variation of offsets e and f with the transmission ratio, respectively. Again, similar to the case of link length c neglecting a few outliers, fixed values of e and f can be obtained. Value of e can be chosen as very low value (lower bound) and value of f can be fixed at 50 mm.

The plot of optimal offset l versus second objective function are shown in Fig. 25. As nearly all the population is concentrated at the upper bound of l, the optimal value of l can be taken as its upper bound value, ie. 300 mm. The joint angle δ varies between 2 to 2.5 radians as shown in Fig. 26. No definite relationship can be obtained between δ and F_2.

Case D: parallel modeling for both electrical and mechanical domains The optimization results (non-dominated solutions) for the modelling of case D is shown in Fig. 27.

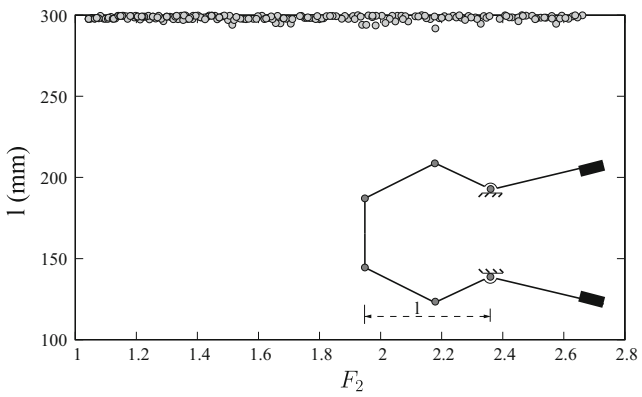

Fig. 25 Variation of offset l with the second objective function (force transformation ratio)

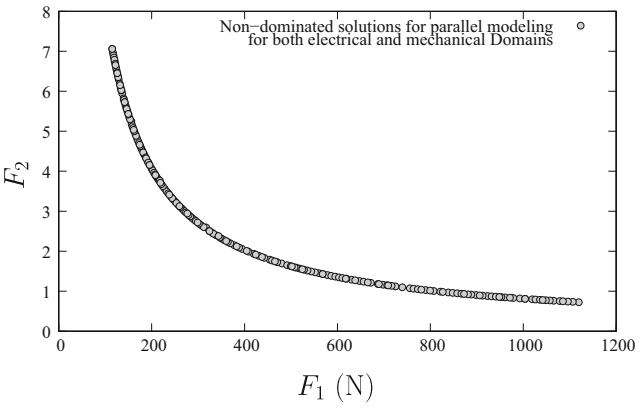

Fig. 27 Non-dominated solutions obtained using NSGA-II for both parallel modeling for both electrical and mechanical domains

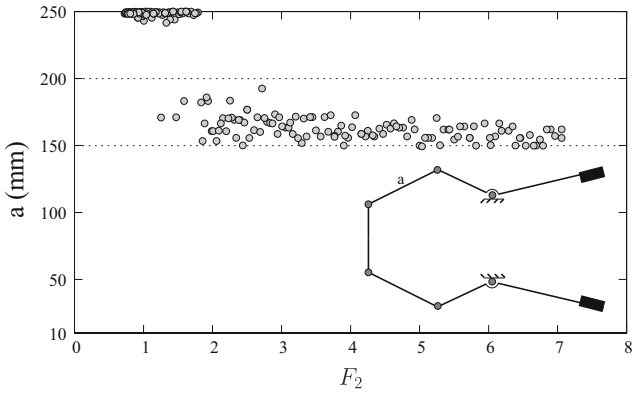

Fig. 28 Variation of link length a with the second objective function (force transformation ratio)

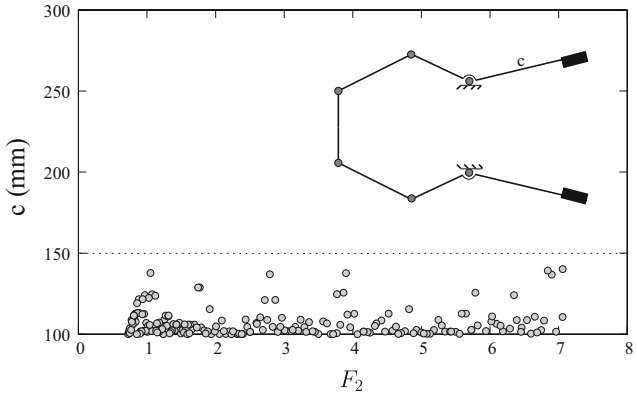

Fig. 30 Variation of link length c with the second objective function (force transformation ratio)

4.0.4 Innovization study

The *innovization study* results are shown in Figs. 28, 29, 30, 31, 32, 33 to 34. The optimal link length a lies in two regions. For a low force transformation ratio, link length a must be fixed at its upper bound (250 mm). However, for a high force transformation ration it should be fixed between 150 mm - 200 mm.

Figure 29 depicts that link length b must be decreased with the increase of force transformation ratio. The value of b must be fixed between (110-220) mm. An inverse relationship exists between link length b and force transformation ratio. Figure 30 confirms that link length c lies between 100 mm - 150 mm for all non-dominated solutions shown in Fig. 27. It can be fixed to its lower bound i.e. 100 mm (the small variation is neglected).

Figure 31 shows that the value of offset e is scattered over the range of (0-35) mm. Figure 31 also shows that no definite relationship exist between link length e with force transformation ratio.

Figure 32 shows the plots of variation of offset f with the transmission ratio. The value of f varies in two ranges, viz. between (10-35) mm and (80-100) mm. Apart from the values of force transformation ratio between 1.4 - 1.6, the value of link offset f should lie between (10-35) mm for the whole range of force transmission ratio.

Figure 33 shows that link offset l also lies in two regions. For a low force transformation ratio, l must be fixed between (100 - 140) mm. However, for a higher value of force transformation ratio it must be fixed between 280 mm - 300 mm. Figure 34 depicts that joint angle (δ) must be increased with the increase in force transformation ratio.

5 Discussions and analysis of results

In the present framework, four different assemblies of actuator modelling have been proposed and combined with a multi objective optimization problem to formulate four separate optimization problems. Multi-objective genetic algorithm has been used to solve all the four problems. Four different sets of non-dominated solutions have been obtained from the multi objective optimization study. For all the four cases, generalized PZ models are developed. However,

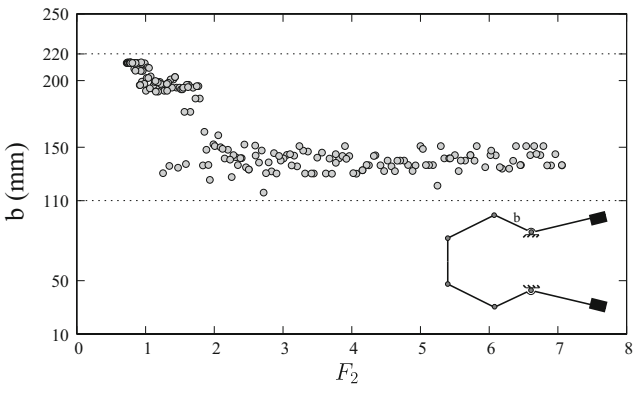

Fig. 29 Variation of link length b with the second objective function (force transformation ratio)

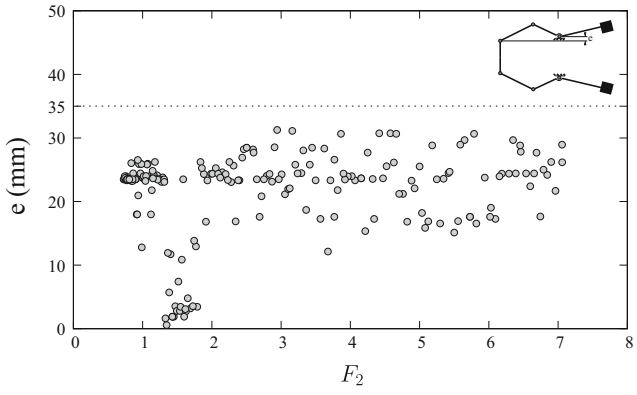

Fig. 31 Variation of offset e with the second objective function (force transformation ratio)

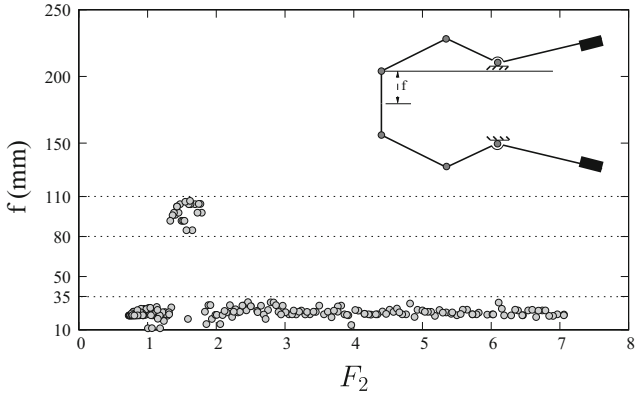

Fig. 32 Variation of offset f with the second objective function (force transformation ratio)

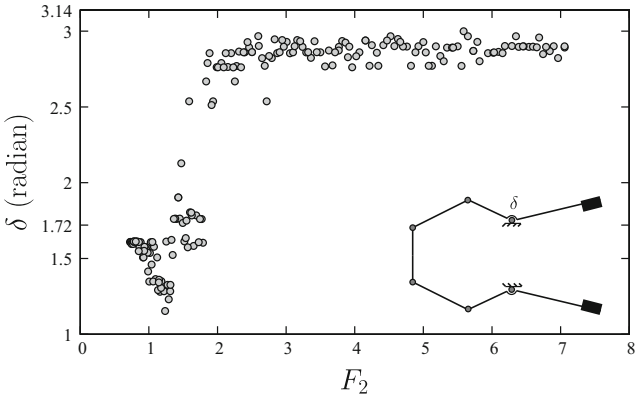

Fig. 34 Variation of joint angle δ with the second objective function (force transformation ratio)

to simplify the model and the multi-objective problem, a simulation was performed and a relation was established between external voltage applied and actuator displacement. The formulated relationship is used in the optimization study for obtaining non-dominated solutions. To distinguish between each model, the obtained non-dominated solutions are shown together in Fig. 35.

As is evident from the figure, among the four cases, case-A is best followed by case-C, case-B and case-D in the respective order for the experimental data set used. Comparing the results with the previous work done by Datta and Deb (2011), we can see significant variations in the two innovization studies. The results of the innovization study discussed in Datta and Deb (2011) are listed in Appendix B. In Datta and Deb (2011), definite relationships between link lengths and force transmission ratio were obtained, which are quite intuitive and straightforward. These relationships represent an ideal case of the gripper design optimization in which the actuator modelling is not considered. However, in real world applications, the specific characteristics of different actuators play a very crucial role in determining the size, applicability and functioning of the mechanisms. In the present work, inclusion of actuator modelling in the optimization study have provided a better insight into this dependency.

Though the relationships obtained in the present work are not very simple and direct, an understanding of the optimal link lengths for the gripper design can be obtained. For example, according to Datta and Deb (2011), the optimal value of link length b is 250 mm. But it can be easily seen from the plots discussed in the present study that the optimal value of link length b is not a fixed number for the entire range of the values of force transmission ratio, rather it shows a significant step variation as the force transmission ratio varies. All significant variations in the results are compared in Table 5 to provide a more comprehensive understanding to the decision maker. The reason of some dicontinuous plots in the innovization study is the infeasibility of solutions.

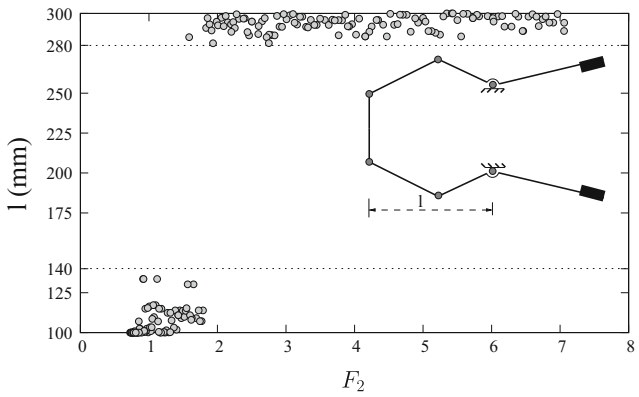

Fig. 33 Variation of offset l with the second objective function (force transformation ratio)

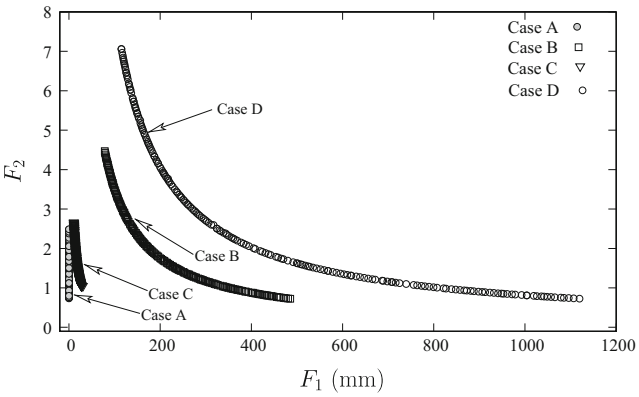

Fig. 35 Comparison of non-dominated solutions obtained using NSGA-II for both series modeling for both electrical and mechanical domains

Table 5 Comparison of results of the present study with the previous study done by Datta and Deb (2011)

Parameter	Datta and Deb (2011)	Case A	Case B	Case C	Case D
Link length a	Upper bound $a = 250$ mm	$a = 250$ mm	Step variation $a = 250$ mm; $F_2 < 1.8$ $a = 160$ mm; $F_2 > 1.8$	No definite result Varies between 197 to 250 mm	Step variation a= 250 mm; $F_2 < 1.8$ a varies 150 to 200 mm; $F_2, > 1.8$
Link length b	Upper bound $b = 250$ mm	No definite result Varies between 150 to 200 mm	No definite result b varies from 190 to 250 mm;$F_2 < 1.8$ b varies from 130 to 160 mm; $F_2 > 1.8$	Line variation Slope = −32.5 Intercept = 165 mm	No definite Varies between 110 to 220 mm
Link length c	Lower bound $c = 100$ mm	Lower bound $c = 100$ mm	Lower bound $c = 100$ mm	Lower bound $c = 100$ mm	No definite result Varies between 100 to 150 mm
Offset e	Lower bound $e = 0$ mm	No definite result e varies from 10 to 20 mm; lower F_2 e varies from 40 to 50 mm; high F_2	No definite result Varies from 0 to 14 mm	Lower bound $e = 0$ mm	No definite result Varies from 0 to 35 mm
Offset f	$f = 37$ mm	No definite result Varies from 25 to 100 mm	No definite result f varies from 15 to 60 mm; $F_2 < 1.25$ and $F_2 > 1.8$ f varies from 90 to 125 mm; $1.25 < F_2 < 1.8$	$f = 50$ mm	No definite result f varies from 10 TO 35 mm; $F_2 < 1.4$ and $F_2 > 1.6$ f varies from 80 to 110 mm; $1.4 < F_2 < 1.6$
Offset l	Lower bound $l = 100$ mm	Lower bound $l = 100$ mm	Step variation $l = 100$ mm;$F_2 < 1.8$ $l = 300$ mm; $F_2 > 1.8$	Upper bound $l = 300$ mm	Step variation l varies from 100 to 140 mm; $F_2 < 1.8$ l varies from 280 to 300 mm; $F_2 > 1.8$
Angle δ	$\delta = 1.72$	No definite result Varies between 1.4 to 2.2	No definite result δ varies from 1.2 to 1.6; $F_2 < 1.25$ δ varies from 1.7 to 2; $1.25 < F_2 < 1.8$ δ varies from 2.5 to 2.8; $F_2 > 1.8$	No definite result Varies between 2 to 2.5	No definite result General trend increase in δ with F_2

On similar lines, for different PZ actuators separate experiments can be performed to choose the appropriate model (out of the four proposed) for the actuator and obtain the corresponding relations between V and z. Using the chosen actuator model, the optimization study can be performed. Furthermore, carrying out the innovization studies in all the cases can also provide more insight to the decision maker in deciding the optimal link lengths and joint angles for the gripper based on his/her requirements.

6 Conclusions

The present work tackles the problem of optimizing the design of a PZ actuator driven robotic gripper. It considers four different combinations of series and parallel assembly for PZ actuator modelling. The model uses linearized governing equations for PZ actuators and thus reduces the computational cost for modelling and optimization study. Relationships between force and voltage with point of actuation are considered to derive the governing equations of the model. The relationships are obtained by modeling the connectors of the stack assembly as a connector spring. The derived equations are integrated with a modified formulation of an existing multi-objective design problem of a robot gripper, originally proposed in Osyczka (2002), and solved in the present work.

The robot gripper problem consists of non-linear, non-convex and multi-modal constraints and objective functions. The problem is solved with a evolutionary multi-objective optimization procedure (EMO). Four different sets of non-dominated solutions are obtained from the optimization study. The obtained non-dominated solutions from each cases are plotted separately. An *Innovization* study is carried out for each case to establish a meaningful relationship between force and actuator displacement with the Pareto-optimal solutions. The four non-dominated solutions are jointly plotted to select the best arrangement. The study will be further extended to other smart actuators.

Acknowledgments Part of the work has been jointly supported by the Department of Biotechnology, India and the Swedish Governmental Agency for Innovation Systems.

Appendix A: Problem formulation

A.1 Design variables

In the optimization process, seven design variables have been considered (same as original study (Osyczka 2002)), consists of link lengths, offsets and joint angle: $\mathbf{x} = (a, b, c, e, f, l, \delta)^T$, where a, b, c denote the link lengths, e, f, l denote link offsets and the joint angle between elements b and c is δ. A sketch of the gripper design is shown in Fig. 1.

A. 2 Problem formulation

The multi-objective problem for the optimization study can be formulated by integrating the the actuator modelling part with the original problem formulation. In this section, the problem formulation is discussed in detail.

A.2.1 Force analysis

In a two dimensional mechanism, bending of the link attached to actuator is avoided as the actuator can undergo translational motion to adjust the stresses. Hence, this link can be treated as a truss element. The force balance on link1 is as shown in Fig. 36.

The structure is in static equilibrium, therefore equating horizontal forces to obtain

$$\frac{P}{2} = RR \times \cos(\alpha). \tag{35}$$

where RR is the reaction force on link a and the actuating force applied by the actuator on the gripper is given by P.

Rearranging above equation

$$RR = \frac{P}{2 \times \cos\alpha}. \tag{36}$$

In Fig. 37, link 2 and 3 are shown with point C hinged. Taking moment equilibrium at C

$$\sum M_{xC} = 0, \tag{37}$$

$$RR \times \sin(\alpha + \beta) \times b = F_k \times c, \tag{38}$$

$$F_k = \frac{RR \times \sin(\alpha + \beta) \times b}{c}, \tag{39}$$

$$F_k = \frac{P \times b \sin(\alpha + \beta)}{2 \times c \cos\alpha}. \tag{40}$$

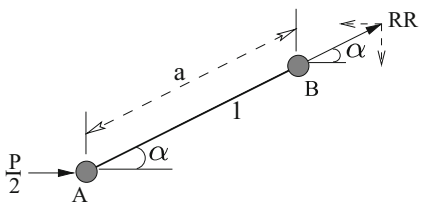

Fig. 36 Free Body Diagram (FBD) of link1 of robot gripper. The actuator force, P, can be divided into two equal forces acting separately on point A and F (point F is shown in Fig. 1, which is a mirror image of point A). RR is the reaction force at point B

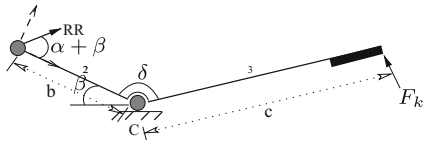

Fig. 37 Free Body Diagram (FBD) of link 2 of robot gripper

A.2.2 Link geometry analysis

From Pythagoras theorem, in Δ ACD (Fig. 38), we get

$$g^2 = (l-z)^2 + e^2,$$
$$g = \sqrt{(l-z)^2 + e^2}.$$

Using cosine law in Δ ABC

$$\cos(\alpha - \phi) = \left(\frac{a^2 + g^2 - b^2}{2 \times a \times g}\right).$$

Solving the above equation for α, we get,

$$\alpha = \arccos\left(\frac{a^2 + g^2 - b^2}{2 \times a \times g}\right) + \phi.$$

Again, from cosine law in Δ ABC, for angle $(\beta + \phi)$

$$\cos(\beta + \phi) = \left(\frac{b^2 + g^2 - a^2}{2 \times b \times g}\right).$$

Solving the above equation for β, we get,

$$\beta = \arccos\left(\frac{b^2 + g^2 - a^2}{2 \times b \times g}\right) - \phi.$$

Also, from Δ ACD we can get

$$\phi = \arctan\left(\frac{e}{l-z}\right).$$

A.3 Constraints

The gripper configuration is physically constrained at various points, for obtaining the required movement. These physical restrictions can be represented in the formulation as the problem constraints.These formulated constraints are multi-modal and non-linear in nature. The formulated constraints for the study are discussed in detail as following:

1. At the maximum actuator displacement, the distance between both ends of the gripper should be less than minimal dimension of the object, for proper gripping.

$$g_1(\mathbf{x}) = Y_{\min} - y(\mathbf{x}, Z_{\max}) \geq 0. \tag{41}$$

in the above equation, $y(\mathbf{x}, z) = 2 \times [e + f + c \times \sin(\beta + \delta)]$ denotes the distance between two ends of the gripper and $Y_{\min}$ is the minimal dimension of the object to be gripped. The parameter $Z_{\max}$ corresponds to the maximum actuator displacement.
2. The distance between gripper ends for maximum actuator displacement (Z_{max}) should be greater than zero:

$$g_2(\mathbf{x}) = y(\mathbf{x}, Z_{\max}) \geq 0. \tag{42}$$

3. When the actuator displacement is zero, the distance between two ends of the gripper should be greater than the maximum dimension object to be gripped.

$$g_3(\mathbf{x}) = y(\mathbf{x}, 0) - Y_{\max} \geq 0. \tag{43}$$

where $Y_{\max}$ denotes the maximum dimension of the object to be gripped.
4. The maximum range of the displacement of the gripping ends of the gripper should be greater than or equal to the distance between the gripping ends corresponding to zero actuator displacement:

$$g_4(\mathbf{x}) = Y_G - y(\mathbf{x}, 0) \geq 0. \tag{44}$$

where Y_G is the maximum displacement that gripper ends can attain.
5. Geometric constraints for the gripper mechanism can be given as:

$$g_5(\mathbf{x}) = (a+b)^2 - l^2 - e^2 \geq 0. \tag{45}$$

The geometric interpretation of constraint $g_5(\mathbf{x})$ is shown in Fig. 39.

$$g_6(\mathbf{x}) = (l - Z_{\max})^2 + (a-e)^2 - b^2 \geq 0. \tag{46}$$

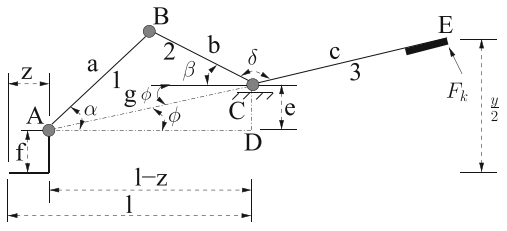

Fig. 38 Geometrical construction for the gripper mechanism. In Δ ACD, g is the hypotenuse distance between point A and point C and ϕ is the angle between AC and AD

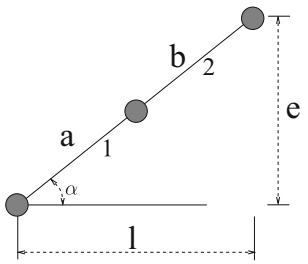

Fig. 39 Geometric illustration of constraint $g_5(\mathbf{x})$ for robot gripper design

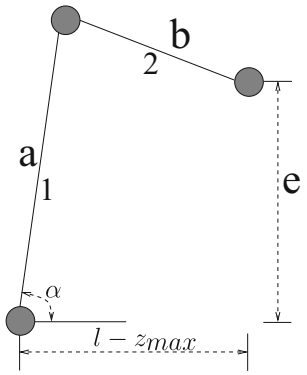

Fig. 40 Geometric illustration of constraint $g_6(\mathbf{x})$

The geometric interpretation of constraint $g_6(\mathbf{x})$ can be seen from Fig. 40.

$$g_7(\mathbf{x}) = l - Z_{\max} \geq 0. \tag{47}$$

6. Minimum force to grip the object should be greater than or equal to chosen limiting gripping force:

$$g_8(\mathbf{x}) = \min_z F_k(\mathbf{x}, z) - FG \geq 0, \tag{48}$$

where FG is the assumed minimal griping force.

A.4 Objective functions

The objective functions for an optimized gripper design, have to be formulated based on link geometry analysis. The formulated functions used in this optimization study are as follows:

1. For any gripper mechanism, the most crucial aspect is to ensure a steady firm grip on the object to be gripped. Hence, the first objective function must be formulated in a way such that this requirement is addressed. We have assumed the difference between the maximum and minimum value of gripping force that will be applied on the object during the whole operation, as our first objective function.

$$F_1(\mathbf{x}) = \max_z F_k(\mathbf{x}, z) - \min_z F_k(\mathbf{x}, z). \tag{49}$$

2. One of the most desirable characteristic in any mechanism, is to have a low energy consumption. In a gripper mechanism, lower power consumption can be ensured by having a higher force transformation ratio. Hence, the second objective function for the present study is formulated as to maximize the force transformation ratio of the mechanism. Force transformation ratio in the initial study was defined as the ratio between the applied actuating force P and the resulting minimum gripping force at the tip of link c (Osyczka (2002)):

$$F_2(\mathbf{x}) = \frac{P}{\min_z F_k(\mathbf{x}, z)}. \tag{50}$$

However, as actuator modelling is taken in consideration in the present study, the actuator force P is no

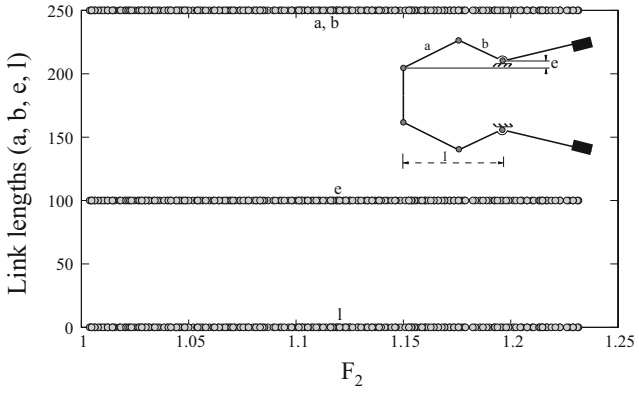

Fig. 41 Variation of link length a, b and offsets e, l with force transformation ratio

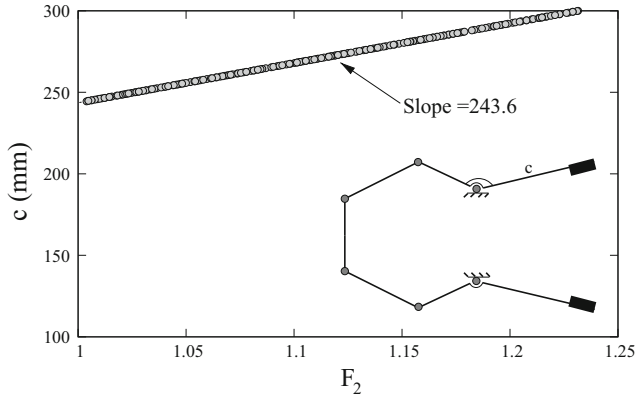

Fig. 42 Variation of offset c with force transformation ratio

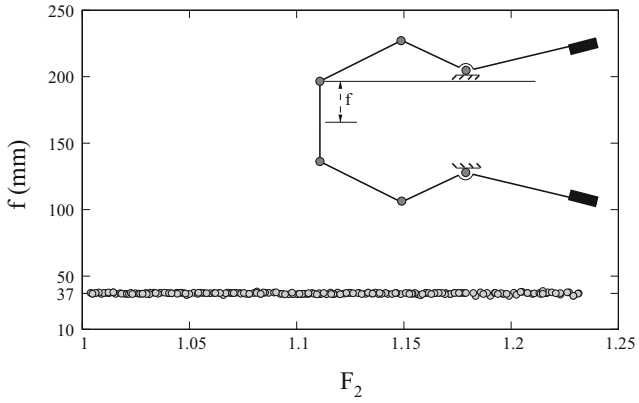

Fig. 43 Variation of offset f with force transformation ratio

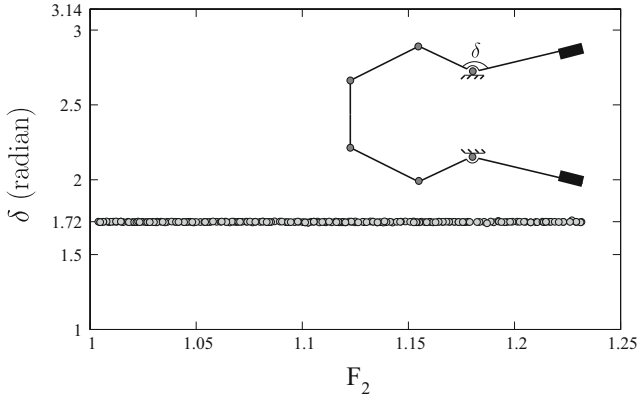

Fig. 44 Variation of joint angle δ with force transformation ratio

longer a constant and varies with actuator displacement. The second modified objective can be defined as

$$F_2(\mathbf{x}) = \max_z \left(\frac{P(\mathbf{x}, z)}{F_k(\mathbf{x}, z)} \right). \tag{51}$$

Appendix B: Previous results

The results of the innovization study done by Datta and Deb (2011) are presented in this appendix. For better understanding and interpretation of the results, corresponding link lengths, link offsets and joint angle are also shown along with the plots. Figure 41 shows the relationships between link lengths a, b and offsets e, l with force transformation ratio (F_2). It is clear from the figure that a and b must be fixed at 250 mm, e must be 100 mm where as l should be 0 mm.

Link length c varies with F_2 as a straight line with slope = 243.6 and intercept = 0, as shown in Fig. 42. Figures 43 and 44 shows that f must be fixed at 37 mm and δ should be 1.72 radian.

References

Adriaens H, De Koning W, Banning R (2000) Modeling piezoelectric actuators. IEEE/ASME Transactions on Mechatronics 5(4):331–341

Anton SR, Sodano HA (2007) A review of power harvesting using piezoelectric materials (2003–2006). Smart Mater Struct 16(3):R1

Benjeddou A (2000) Advances in piezoelectric finite element modeling of adaptive structural elements: a survey. Comput Struct 76(1):347–363

Bicchi A, Kumar V (2000) Robotic grasping and contact: A review. In: ICRA. Citeseer, pp 348–353

Chee CY, Tong L, Steven GP (1998) A review on the modelling of piezoelectric sensors and actuators incorporated in intelligent structures. J Intell Mater Syst Struct 9(1):3–19

Ciocarlie M, Allen P (2010) Data-driven optimization for underactuated robotic hands. In: IEEE International Conference on Robotics and Automation (ICRA), 2010. IEEE, pp 1292–1299

Ciocarlie M, Hicks FM, Holmberg R, Hawke J, Schlicht M, Gee J, Stanford S, Bahadur R (2014) The velo gripper: A versatile single-actuator design for enveloping, parallel and fingertip grasps. Int J Robot Res 33(5):753–767

Croft D, Devasia S (1998) Hysteresis and vibration compensation for piezoactuators. J Guid Control Dyn 21(5):710–717

Datta R, Deb K (2011) Multi-objective design and analysis of robot gripper configurations using an evolutionary-classical approach. In: Proceedings of the 13th annual conference on Genetic and evolutionary computation. ACM, pp 1843–1850

Deb K, Pratap A, Agarwal S, Meyarivan T (2002) A fast and elitist multiobjective genetic algorithm: Nsga-ii. IEEE Trans Evol Comput 6(2):182–197

Deb K, Srinivasan A (2006) Innovization: Innovating design principles through optimization. In: Proceedings of the 8th annual conference on Genetic and evolutionary computation. ACM, pp 1629–1636

Goldfarb M, Celanovic N (1999) A flexure-based gripper for small-scale manipulation. Robotica 17(02):181–187

Gu G-Y, Zhu L-M, Su C-Y, Ding H (2013) Motion control of piezoelectric positioning stages: modeling, controller design, and experimental evaluation. IEEE/ASME Transactions on Mechatronics 18(5):1459–1471

Harres D (2013) MSP430-based robot applications: a guide to developing embedded systems. Newnes

IEEE standard (1987) I.E.E.E. Standard on Piezoelectricity: An American National Standard. I.E.E.E. Transactions on sonics and ultrasonics. IEEE

Irschik H (2002) A review on static and dynamic shape control of structures by piezoelectric actuation. Eng Struct 24(1):5–11

Jain A, Datta R, Bhattacharya B (2015) Unified minimalistic modelling of piezoelectric stack actuators for engineering applications. In: Robot Intelligence Technology and Applications 3. Springer, pp 459–473

Krenich S (2004) Multicriteria design optimization of robot gripper mechanisms. In: IUTAM Symposium on Evolutionary Methods in Mechanics. Springer, pp 207–218

Low T, Guo W (1995) Modeling of a three-layer piezoelectric bimorph beam with hysteresis. J Microelectromech Syst 4(4):230–237

Osyczka A (2002) Evolutionary algorithms for single and multicriteria design optimization. Physica-Verlag, Heidelberg

Osyczka A, Krenich S, Karas K (1999) Optimum design of robot grippers using genetic algorithms. In: Proceedings of the Third World Congress of Structural and Multidisciplinary Optimization (WCSMO), Buffalo, New York, pp 241–243

Pérez R, Agnus J, Clévy C, Hubert A, Chaillet N (2005) Modeling, fabrication, and validation of a high-performance 2-dof piezoactuator for micromanipulation. IEEE/ASME Transactions on Mechatronics 10(2):161–171

Reddy PVP, Suresh VS (2013) A review on importance of universal gripper in industrial robot applications

Saravanan R, Ramabalan S, Ebenezer N, Dharmaraja C (2009) Evolutionary multi criteria design optimization of robot grippers. Appl Soft Comput 9(1):159–172

Shikhar P (2014) Analysis and design optimization of a seven link robot gripper with an integrated actuation system. Master's thesis, IIT Kanpur

Tzen J-J, Jeng S-L, Chieng W-H (2003) Modeling of piezoelectric actuator for compensation and controller design. Precis Eng 27(1):70–86

Zubir MNM, Shirinzadeh B, Tian Y (2009) Development of a novel flexure-based microgripper for high precision micro-object manipulation. Sensors Actuators A Phys 150(2):257–266